Polymer Bulletin 31, 495–501 (1993)

Polymer Bulletin

Comparison of the failure mode in short and long glass fiber-reinforced injection-molded polypropylene composites by acoustic emission

T. Czigány[1] and J. Karger-Kocsis[2,*]

[1]Institute for Machine Part Design, Technical University of Budapest, H-1111 Budapest, Hungary
[2]Institut für Verbundwerkstoffe GmbH, Universität Kaiserslautern, Postfach 3049, D-67663 Kaiserslautern, Germany

ABSTRACT

The failure mode in injection-molded short (SGF) and long glass fiber (LGF) reinforced polypropylene (PP) was studied on compact tension (CT) specimens simultaneously by acoustic emission (AE) and transmitted light microscopy. A significant difference was revealed in the failure manner characterized by the cumulative run, amplitude and energy distribution curves between the SGF- and LGF-PP both in the crack initiation and propagation stage. It was established that the failure of SGF-PP did not alter with the loading; this composite failed mostly by matrix deformation along with fiber/matrix debonding and some fiber pull-out. The failure mode of the LGF-PP differed from that scenario, since fiber fracture was resolved in every stage of the loading. On the contrary to SGF-PP, the failure of this composite was governed by fiber-related events (fracture, pull-out, debonding). The amplitude and energy of the AE signals were assigned to individual failure events and thus the failure sequence concluded.

1. INTRODUCTION

The development of discontinuous fiber reinforced, injection-moldable composites can be characterized by a steady increase in the aspect ratio (l/d) of the reinforcement in the molded items [1]. By special pultrusion techniques it was achieved recently that the length of the reinforcing fibers agrees with that of the injection-moldable granules (generally <10 mm) [2]. Tough there is some degradation in the aspect ratio due to the molding process [1], the overall enhancement of l/d yields better stiffness and strength values, especially when the fibers are aligned into the loading direction [2]. An analogous improvement is , however, not obvious in respect with the toughness, since the energy dissipated by various mechanisms (fiber/matrix debonding, fiber pull-out, fiber fracture) differs from one another [3-4]. In addition, a change in the above events, affects the matrix failure, as well, so the toughness performance can hardly be predicted. It is difficult to make any firm statement on the relative occurrence of the fiber-related failure events based on post-mortem fractographic analysis; therefore the use of in-situ failure monitoring techniques, such as acoustic emission (AE), is preferred. This technique is very beneficial due to the fact that AE signal characteristics can be assigned to given individual failure events with high reliability [5]. In the knowledge of the failure mode the toughness of the composites can be estimated and thus "tailored" upon request. This approach sollicitates the development of composites targeting an improved balance between stiffness, strength and toughness values.

Aim of this contribution is to compare the failure mode of short and long glass fiber (SGF and LGF, respectively) reinforced, injection-molded polypropylene (PP) composites by in-situ monitoring of the fracture process using light microscopy and AE technique at the same time.

2. EXPERIMENTAL

2.1. Materials, Specimens

Large compact tension (CT) specimens (notch length, a≈20 mm; free ligament width, W≈50 mm) were cut from molded plaques of about 3 mm thickness. The volume fraction (V_f) of the reinforcement was 0.083 (=20 wt.%). The CT-specimens were designated as L-T according to the ASTM E 616-81 standard being notched transversal (T) to the mold filling

*Corresponding author

(MFD) direction, i.e. their loading occurred longitudinal (L) to the MFD. The microstructure of the molded plaques, including the fiber layering and mean fiber orientation in the separated layers, was described elsewhere [6-7].

2.2. Tests

Loading of the CT-specimens was performed on a Zwick 1445 type tensile machine at ambient temperature (RT) and at v=1 mm/min crosshead speed. The failure behavior of the CT- specimens was studied in-situ by a traveling light microscope. The AE events of the specimens were also collected by an AE-transducer during the loading. AE was detected by a Defektophone NEZ 220 analyzer (Central Research Institute for Physics, Budapest, H) using wide bandwith transducers (20-1000 kHz) with built-in preamplifier. The signals were further amplified logarithmically. During the tests the following primary AE signals were acquisited: elapsed time, ringdown count, rise time, event duration, peak amplitude, number of events.

3. RESULTS AND DISCUSSION

3.1. Fracture Behavior

Figures 1 and 2 show the force-load line displacement (F-v_{LL}) curves of a CT-specimen along with the course of the cumulative AE events and series of microphotographs taken during the loading for SGF- and LGF-PP, respectively. The F-v_{LL} curves were sectioned (cf. I to III in Figures 1 and 2) in order to get information on the failure sequence by differentiating among the AE signals collected.

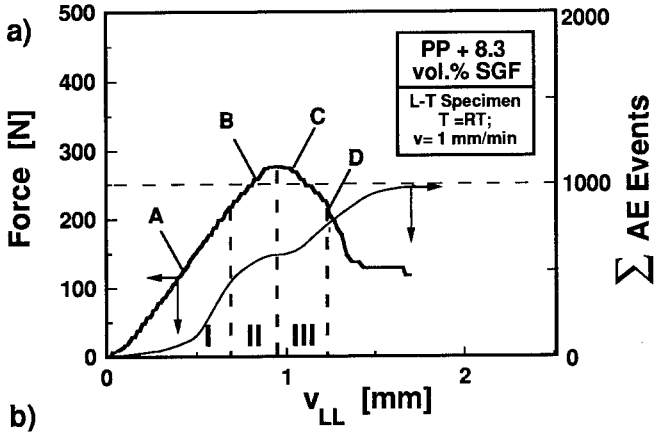

Figure 1
F-v_{LL} curve of the CT-specimen, cumulative run of the AE events (a) and serial micro-photographs taken from the crack growth during loading (b) in SGF-PP.
(Figure 1a indicates for sectioning of the loading curve for AE signal analysis and for the taking positions of the microscopic pictures given in Figure 1b.)

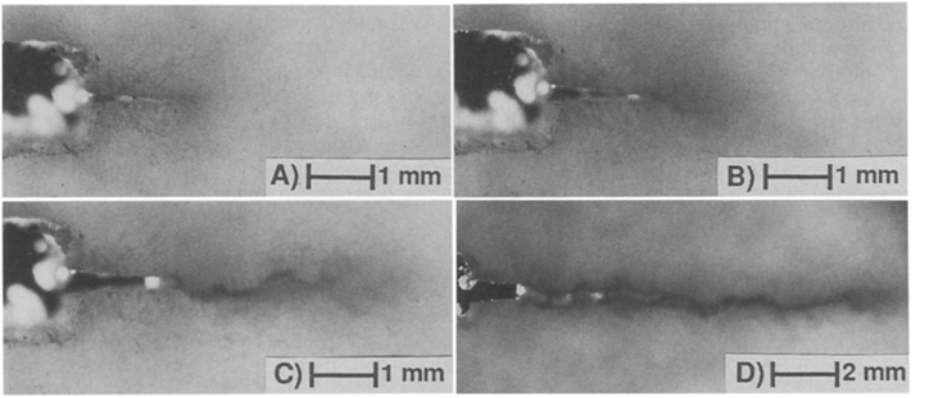

Incorporation of LGF into the PP matrix instead of SGF increases the maximum load and thus the fracture toughness of the composite, as well (K_C wass enhanced from 3.0 to 4.4 MPam$^{1/2}$ in this case). Both the course and the sum of the AE events differ considerably for the SGF- and LGF-PP indicating for basic differences in the failure manner (cf. Figure 1a and 2a).

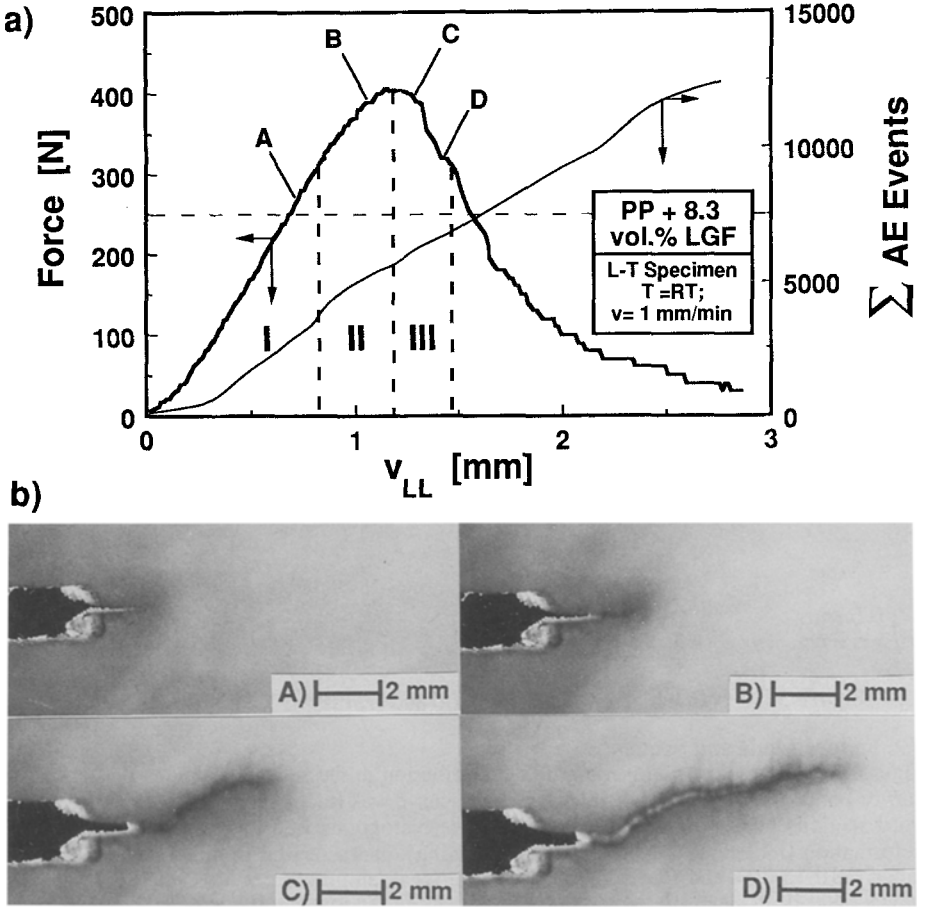

Figure 2 F-v_{LL} curve of the CT-specimen, cumulative run of the AE events (a) and serial microphotographs taken from the crack growth during loading (b) in LGF-PP.

Considering the related light microscopic pictures (Figures 1b and 2b) one can state that the crack propagation starts before the maximum load is reached (cf. pictures B in both Figures 1b and 2b). This quite surprising result hints that the size of the damage zone (an thus the resistance to crack growth) changes during the loading. It was recently reported that the development of the damage zone depends on both microstructural (such as fiber structuring, l/d ratio) and testing parameters (e.g. load level, strain rate) [8]. The crack growth behavior of such composites can be more adequately represented by the resistance (R) curve, determined by the single specimen technique (i.e. K_C increment with the crack propagation, a_i/W, where "a_i" is the actual crack length and W is the ligament width of the specimen). The zig-zag type crack growth profile in SGF-PP reflects that the fiber avoidance mechanism dominates in L-T specimens, where GFs are aligned into the loading direction in the surface layers. Such a

crack profile is not characteristic for LGF-PP due to the very high GF aspect ratio. The direction of the crack growth generally deviates from the anticipated one which is in plane with the razor blade notching. From the first step in the crack deviation path (pictures C and D in Figure 2b), caused by fiber avoidance, one could conclude that the mean fiber pull-out length is of about 1 mm. This corresponds to a critical fiber length of > 2mm, which agrees exactly with that value derived from fractographic analysis of fatigue fractured specimens [9]. The improved stress transfer capability of LGF is envisaged in Figure 3 comparing the crack tip regions developed in SGF- and LGF-PP, respectively. Stress concentration at the fiber ends (SGF) and along a longer fiber section (LGF) gives rise of crazing in the given PP which promotes fiber/matrix debonding. The extension of the damage zone is more pronounced in LGF-, than in SGF-PP. The craze bands (running perpendicular to the loading direction) and debonded fibers within this stress-whitened damage zone (becoming dark in the pictures) are clearly discernible in Figure 3. The final crack path emerges by interconnection of the different crazed planes due to further fiber debonding, pull-out and fracture events with concomitant matrix deformation. It will be shown later that the matrix deformation is crucial in SGF-PP, while plays a role of second order in LGF-PP.

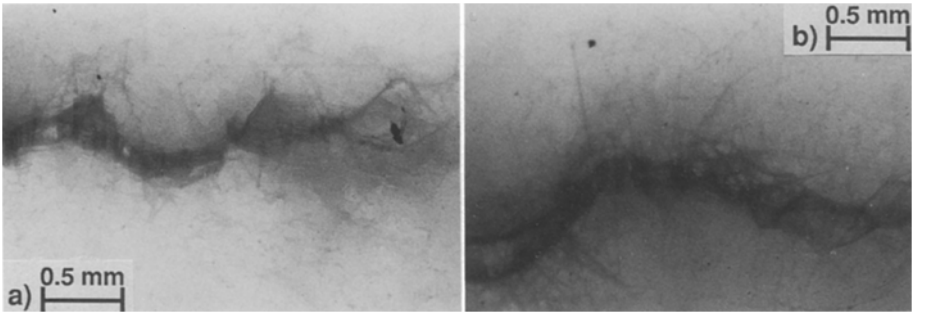

Figure 3 Crack tip region of SGF- (a) and LGF-PP (b) at high crack growth.

3.2. Failure Mode and Sequence

Figure 4 compares the relative amplitude distribution in the selected sections of the F-v_{LL} curves both for SGF- and LGF-PP. The F-v_{LL} curve was fractionated that both the first and third section ended at $0.8F_{max}$. The amplitude histograms in SGF-PP reflect that matrix deformation (including crazing and shear yielding), characterized by the lowest amplitude range (≈10-15 dB), and fiber/matrix debonding (peak amplitudes:20 to 35 dB) dominate in stages I and II. In stage III, the increased frequency of the low amplitude AE events indicates for a more pronounced matrix deformation. This is a clear evidence that crack propagates when matrix ligaments separating previously failed sites within the damage zone (craze bands, debonded fiber surfaces etc.) rupture by plastic deformation. This process can be termed therefore as "damage coalescence".

Based on Figure 4b, the failure mode is completely different for the LGF-PP. The AE signals with an amplitude beween 45 and 70 dB in stage I can be ascribed to long range debonding and pull-out events. This remains the main failure manner up to F_{max}, with the only exception that debonding (peak amplitudes: 45-50 dB) and pull-out (amplitude≈ 60 dB) separate from one another. The other basic difference between the SGF and LGF-reinforcement, that in presence of the latter fiber fracture can be resolved (peak amplitude: 80-85 dB) in every stage of the loading. This mechanism becomes, however, more affirmative when the crack advances (cf. stages II and II in Figure 4b). The above concluded failure modes are in good agreement with those derived from the corresponding light microscopic pictures.

Discrimination according to the energy of the AE events may deliver further useful information about the failure process. Figure 5a emphasizes that the failure mode of SGF-PP in the whole loading range is the same. The slight shift in the energy histograms toward lower values in the crack propagation phase can be attributed to the damage coalescence process discussed above. The failure is governed by matrix deformation (energy:10^{-9}...10^{-11} pJ), fiber/matrix debonding (energy:10^{-7}...10^{-8} pJ). The events of higher acoustic energy ($\approx 10^{-4}$ pJ) are related to fiber pull-out, which occurs mostly in the crack propagation phase (stage III in Figure 5a).

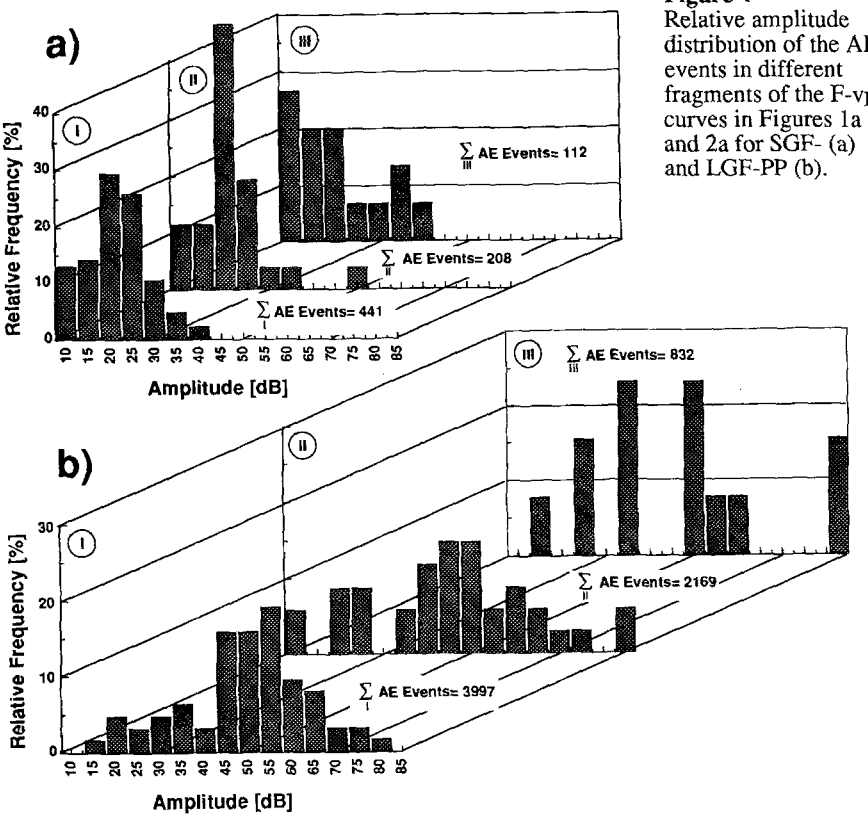

Figure 4
Relative amplitude distribution of the AE events in different fragments of the F-v_{LL} curves in Figures 1a and 2a for SGF- (a) and LGF-PP (b).

In the more stiff LGF-PP fiber fracture (energy:10^{-2}...10^{-1} pJ) and pull-out (energy:10^{-3}... 10^{-4} pJ) dominate both in the crack initiation (I) and early crack propagation (II) stage (Figure 5b). Matrix deformation can be revealed in stages II and III, where crack growth is necessarily linked to a breaking-up process of the matrix ligaments. In the crack propagation phase the fiber-related failure events (debonding, pull-out, fracture) are well separated from one another and also from the matrix. This is believed to reflect a change in the matrix deformation which becomes sligthly more brittle. Instead of plastic flow, crazing and matrix fracture occur, the energy of which lays somewhat higher than of ductile tearing (cf. stages II in Figure 5a and 5b). This matrix "embrittlement", caused by the speed increase in the crack growth phase, is strongly affected by the fiber content (V_f) and especially by the local fiber

in Figure 5a and 5b). This matrix "embrittlement", caused by the speed increase in the crack growth phase, is strongly affected by the fiber amount (V_f) and especially by the local fiber layering [10]. It should be noted here that the ductile-plastic type deformation of the matrix yields the overlapping ("smearing") of the AE signals generated by different fiber-related failure events.
The above described assignment of the AE events corroborates our previous findings deduced for glass strand mat reinforced polyamides [11-12].

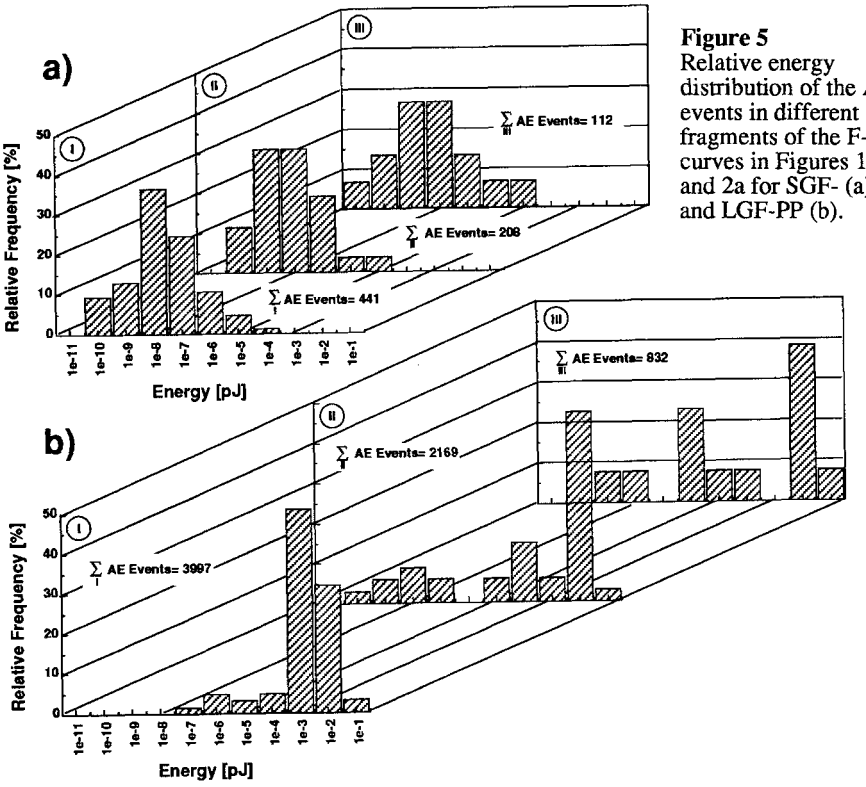

Figure 5
Relative energy distribution of the AE events in different fragments of the F-v_{LL} curves in Figures 1a and 2a for SGF- (a) and LGF-PP (b).

As shown above, the AE amplitude and energy discrimination methods are useful tools for distinguishing among various failure manners in different phases of the mechanical laoding. In the knowledge of the failure mode and sequence, the dissipation of the mechanical energy can be estimated and thus composites of improved mechanical property profile can be produced.

4. CONCLUSIONS

The failure mode, caused by monotonic increased loading, was studied in chopped short (SGF) and long glass fiber (LGF) reinforced injection-molded polypropylene (PP) by simultaneous light microscopic and acoustic emission (AE) monitoring. The individual failure events could be correlated with those of the AE when the amplitude and energy of the AE

The failure mode was the same in the crack initiation and propagation stages in SGF-PP (matrix deformation, fiber/matrix debonding). In addition, practically no change in their relative occurrence was noticed with the loading.
In case of the LGF-PP fiber fracture, pull-out and debonding processes took place. Based on their AE signal parameters (amplitude, energy) these fiber-related events were discriminated in different stages of the loading.
It was indicated that the relative contribution of the individual failure manners to the (fracture) toughness of the composite can be estimated by the AE technique. In addition, this technique seems to work well also when effects of fiber/matrix coupling are under consideration [13-14].

ACKNOWLEDGEMENT
This work was performed in frame of the DFG Project "GMT-Verbundwerkstoffe".

REFERENCES

1 J. Karger-Kocsis: Structure and fracture mechanics of injection-molded composites in "International Encyclopedia of Composites" Vol.5, (Ed.: S. M. Lee), VCH, N.Y., 1991, pp. 337-356
2 J. M. Crosby: Long-fiber molding materials, Ch.5 in "Thermoplastic Composite Materials", (Ed.: L. A. Carlsson), Elsevier, Amsterdam, 1991, pp. 139-165
3 V. B. Gupta, R .K. Mittal and M. Goel: Compos.Sci.Technol., **37** (1990), 353-369
4 J.-K. Kim and Y.-W. Mai: ibid., **41** (1991), 333-378
5 H. Hansmann: Materialprüfung, **33** (1991), 304-309
6 D. E. Spahr, K. Friedrich, J. M. Schultz and R. S. Bailey: J.Mater.Sci., **25** (1990), 4427-4439
7 J. Karger-Kocsis: Compos.Sci.Technol., (1993) (in press)
8 Idem: Microstructural aspects of fracture in polypropylene and in its filled, chopped fiber and fiber mat-reinforced composites, Ch. 3.4. in "Polypropylene: Structure, Blends and Composites", (Ed.:J.Karger-Kocsis), Chapman and Hall, London, 1994 (to appear)
9 J. Karger-Kocsis, K. Friedrich and R. S. Bailey: Adv.Compos.Mater., **1** (1991), 103-121
10 J. Karger-Kocsis: J.Polym.Eng., **12** (1993), 77-107
11 J. Karger-Kocsis, Q.Yuan and T.Czigány: Polym.Bull., **28** (1992), 717-723
12 J. Karger-Kocsis and T.Czigány: J.Mater.Sci., **28** (1993), 2438-2448
13 J. Bohse: Kunststoffe, **82** (1992), 72-76
14 J. Bohse and G. Kroh: J.Mater.Sci., **27** (1992), 298-306

Accepted August 3, 1993 C